

Factors affecting the quality of XBT data – results of analyses on profiles from the Western Mediterranean Sea

F. Reseghetti¹, M. Borghini², and G. M. R. Manzella³

¹ENEA-ACS-CLIM-MED, Forte S. Teresa – Pozzuolo di Lerici, 19032 Lerici (Sp), Italia

²CNR-ISMAR, Sez. Oceanografia Fisica, Forte S. Teresa – Pozzuolo di Lerici, 19032 Lerici (Sp), Italia

³ENEA-ACS, Forte S. Teresa – Pozzuolo di Lerici, 19032 Lerici (Sp), Italia

Received: 5 May 2006 – Published in Ocean Sci. Discuss.: 1 September 2006

Revised: 29 November 2006 – Accepted: 2 February 2007 – Published: 8 February 2007

Abstract. EXpendable BathyThermograph (XBT) temperature profiles collected in the framework of the Mediterranean Forecasting System – Toward Environmental Prediction (MFS-TEP) project have been compared with CTD measurements. New procedures for the quality control of recorded values have been developed and checked. Some sources of possible uncertainties and errors, such as the response time of the apparatus (XBT probe, thermistor and readout chain), or the influence of initial conditions are also analysed. To deal with the high homogeneity of Mediterranean waters, a new technique to compute the fall rate coefficients, that give a better reproduction of the depth of thermal structures, has been proposed, and new customized coefficients have been calculated. After the application of a temperature correction, the overall uncertainties in depth and in temperature measurements have been estimated.

1 Introduction

Since the 60's, XBT probes have been successfully adopted by oceanographers as an easy way to collect temperature profiles by using commercial ships (Ship Of Opportunity Programs – SOOP). Different types of probes are available: T4, T5, T6, T7, Deep Blue (DB), Fast Deep (FD) etc., and their characteristics are reviewed in several “Cookbooks”, e.g. Sy (1991), AODC (1999, 2001 and 2002), Cook and Sy (2001). The choice of the type depends on ship speed and on terminal depth. In Table 1, some properties based on guides produced by the manufacturer (Lockheed Martin Sippican – USA, hereafter Sippican) are detailed. Several analyses on the quality of XBT temperature profiles have been published, and a lot of influencing factors have been identified (Seaver

and Kuleshov, 1982; Green, 1984; Singer, 1990; Hallock and Teague, 1992).

The main problems are the evaluation of the uncertainty in recorded temperature values and the estimate of the depth, which is calculated through a fall rate equation $Z(t)=At-Bt^2$, where Z is the depth at the time t . The coefficients are both positive and depend on XBT types (Table 2).

“ A ” is related to the hydrodynamics characteristics of the probe, and is equivalent to the initial falling speed, “ B ” is a function of the mass variation rate of the probe, and of the variation of seawater properties depending on the depth, such as density and viscosity (e.g. Seaver and Kuleshov, 1982; Green, 1984; Hanawa et al., 1994, 1995).

Since the end of the 70's, some inadequacies were recognised between the computed depths and the values measured by other oceanographic instruments, such as STD or CTD (e.g. McDowell, 1977; Flierl and Robinson, 1977; Fedorov et al., 1978). In 1994, the Integrated Global Ocean Services System (IGOSS) Task Team released a comprehensive report on XBT/CTD comparison and proposed a new computational technique (Hanawa et al., 1994, 1995), derived from the approach implemented by Hanawa and Yasuda (1992). New values for fall rate coefficients for T4/T6/T7/DB probes manufactured by Sippican and TSK (Tsurumi Seiki Co. – Japan) were calculated (see Table 2). The best-fit values for T4/T6 and T7/DB probes are not coincident: such a small discrepancy, even if within the standard deviation, could indicate that the probe motion slightly depends on the XBT type. The error in the depth value was estimated to be 2% of the depth or 5 m, whichever is greater. In spite of the consensus on the IGOSS fall rate coefficients, which were calculated by using data from the major world oceans (but not from the Mediterranean Sea), discrepancies were found in some areas, such as in the Antarctic Ocean (Thadathil et al., 2002).

Analyses of XBT performances in the Mediterranean Sea are not available: it was noted that XBT profiles from the Ligurian Sea have a general agreement with CTD profiles,

Correspondence to: F. Reseghetti
(franco.reseghetti@santateresa.enea.it)

Table 1. Some characteristics of different XBT probes. Nominal maximum speed and experimental range of speed are shown in the first two columns; then, the terminal depth and the correspondent nominal acquisition time AT (as deduced by using IGOSS fall rate coefficients). If the fall rate coefficients proposed by manufacturer are used, the acquisition time for T4/T6 probes is 72.9 s, and 122.5 s for T7/DB probes. The averaged acquisition time ($\langle AT \rangle$) and the correspondent depth calculated following the procedure detailed in Manzella et al. (2003), with the measured range, are quoted. Values concerning T4 and DB probes at $v \geq 20$ kn are based on XBTs dropped on the transect Genova-Palermo. The number of XBT probes in each dataset is added.

XBT Type	Max Speed (kn)	Real Speed (kn)	Depth (m)	AT (s)	$\langle AT \rangle$ (s)	Range (s)	Average Depth (m)	Range (m)	No. XBT
T4	30	0	460	70.5	87.3 \pm 2.0	83.0–90.7	567 \pm 12	540–588	22
T4	30	21–27	460	70.5	80.6 \pm 1.1	76.8–84.9	525 \pm 7	500–552	230
T6	15	\leq 10	460	70.5	85.2 \pm 4.1	77.7–90.5	554 \pm 26	506–587	11
T5	6	4–6	1830	290.5	352.9 \pm 9.7	332.9–362.9	2183 \pm 54	2071–2238	14
T7	15	\leq 15	760	118.3	142.5 \pm 2.2	138.6–150.9	908 \pm 14	884–958	68
T7	15	17	760	118.3	136.3 \pm 1.4	133.2–138.2	870 \pm 9	851–881	15
DB	20	0	760	118.3	143.9 \pm 2.4	139.3–148.5	916 \pm 14	888–944	18
DB	20	\leq 20	760	118.3	140.9 \pm 1.8	126.3–149.6	898 \pm 11	809–951	1312
DB	20	21	760	118.3	137.6 \pm 1.9	136.3–140.5	878 \pm 12	870–896	4
DB	20	22	760	118.3	134.2 \pm 2.2	130.9–140.3	857 \pm 13	837–894	27
DB	20	23	760	118.3	127.5 \pm 2.3	124.3–132.8	817 \pm 14	797–849	35
DB	20	24	760	118.3	122.1 \pm 2.9	115.6–127.0	783 \pm 18	743–813	31
DB	20	25	760	118.3	118.0 \pm 2.3	113.0–123.8	758 \pm 14	727–794	48
DB	20	26	760	118.3	114.2 \pm 2.5	109.3–118.6	735 \pm 15	704–762	37
DB	20	27	760	118.3	111.1 \pm 1.2	109.8–113.5	716 \pm 8	707–730	9

Table 2. Different values for the coefficients of the fall rate equation are compared. IOC proposed Hanawa et al. (1995) values for T4, T6, T7 and DB as official IGOSS fall rate coefficients for such probes. The values obtained from the best fit for specific XBT types are added.

Author	A (ms^{-1})	B (ms^{-2})
Sippican T4/T6/T7/DB	6.472	0.00216
Sippican T5	6.828	0.00182
Sippican FD	6.390	0.00182
Hanawa et al. (1995)	6.691 \pm 0.021	0.00225 \pm 0.00030
T4/T6/T7/DB		
Hanawa et al. (1995)	6.683 \pm 0.033	0.00215 \pm 0.00052
Best fit T4/T6		
Hanawa et al. (1995)	6.701 \pm 0.023	0.00238 \pm 0.00016
Best fit T7/DB		

but some discrepancies occur at the thermocline depth and in correspondence with deep thermal structures (Reseghetti, 2003¹). Consequently, the acquisition of several pairs of co-located and contemporaneous XBT/CTD temperature profiles in the Western Mediterranean Sea was planned within

the Mediterranean Forecasting System – Toward Environmental Prediction (MFS-TEP) project, in order to evaluate XBT performance and to improve experimental procedures and data processing. Thermal structures and their depth have been identified on recorded XBT and CTD temperature profiles, whereas the correspondent dT/dz profiles have offered the opportunity to estimate the capability of the XBT probes in measuring thermal variation. Then, temperature difference profiles ($\Delta T = T(\text{XBT}) - T(\text{CTD})$) have shown the dependence of discrepancy on depth.

New fall rate coefficients and data analysis procedures, that reproduce better the depth of thermal structures, and a new estimate of the temperature uncertainty have been determined. This paper summarizes the results of the activity developed within MFS-TEP and ADRI-COSM (ADRIatic sea integrated COastal areas and river basin Management system pilot project), and is organised as follows: in Sect. 2, XBT and CTD data collection procedures are presented; in Sect. 3, data analysis, including the evaluation of factors influencing the motion of the probe, the quality of measurements and new fall rate coefficients are reviewed; in Sect. 4, the values of the uncertainty in temperature are detailed; comments and final remarks are in Sect. 5.

¹Reseghetti, F.: Comparison between quasi contemporaneous and co-located CTD and XBT measurements, MFS-TEP – VOS Technical Report Nr. 1 (unpublished) available at: <http://moon.santateresa.enea.it/documents/xbtvsctd.pdf>, 2003.

2 Materials and methods

In this paper, the speed of a ship is in knots (kn), and XBT temperatures are in situ values in Celsius degrees ($^{\circ}\text{C}$). CTD profiles are considered the “true” representation of the temperature: the differences between CTD and XBT values are assumed to reflect inaccuracies in the XBT measurements, which are released with three decimal digits, due to the mathematical processing.

2.1 CTD characteristics and its data processing

CTD profiles were recorded using a Sea-Bird SBE 911 *plus* automatic profiler, calibrated before and after each cruise at NURC (NATO Undersea Research Centre, La Spezia – Italia). The adopted falling speed was 1.0ms^{-1} . The apparatus has a 24 Hz sampling rate, with a (static) nominal accuracy of 0.001°C in temperature, and of 0.0003Sm^{-1} in conductivity. The (static) time constants are 0.065 s for the conductivity and temperature sensors (which implies a nominal spatial resolution of 0.065 m), and 0.015 s for the pressure sensor (the spatial resolution is 0.015 m). CTD profiles were processed using standard Seabird’s software (Data Conversion, Alignment, Cell Thermal Mass, Filtering, Derivation of physical values, Bin Average and Splitting); afterwards, they were qualified with Medatlas protocols (Maillard and Fichaut, 2001).

2.2 XBT data acquisition and data processing

Some types of XBT probes manufactured by Sippican in different years were launched during CTD casts from the CNR’s R/V URANIA when the ship was motionless. Different seawater characteristics were found: a weak surface thermocline in May 2003 and in May 2004, a strongly stratified upper layer (down to about 100 m depth) in September 2003 and September–October 2004, and winter-homogenised waters in January 2004. Geographical and temporal co-ordinates for each pair of CTD cast and XBT probe are shown in Fig. 1. Specific analyses and results are concerned with the T4 and DB probes, but a significant part of the conclusions can be extended either to T6 or to T7 probes. The physical properties of T4/T6 and T7/DB pairs of probes are the same, within the probe-to-probe variability, with the length of copper wire on the shipside as the only known difference between T4 and T6, or T7 and DB probes. The data acquisition system consists of Sippican MK-12 readout card, PC with Intel P-II 166 MHz-processor. The XBT sampling rate is 10 Hz, the instrumental sensitivity on temperature is 0.01°C , whereas the uncertainty estimated by the manufacturer is $|\delta T| \sim 0.10^{\circ}\text{C}$. Each XBT probe was dropped within 480 s from the start of a CTD cast.

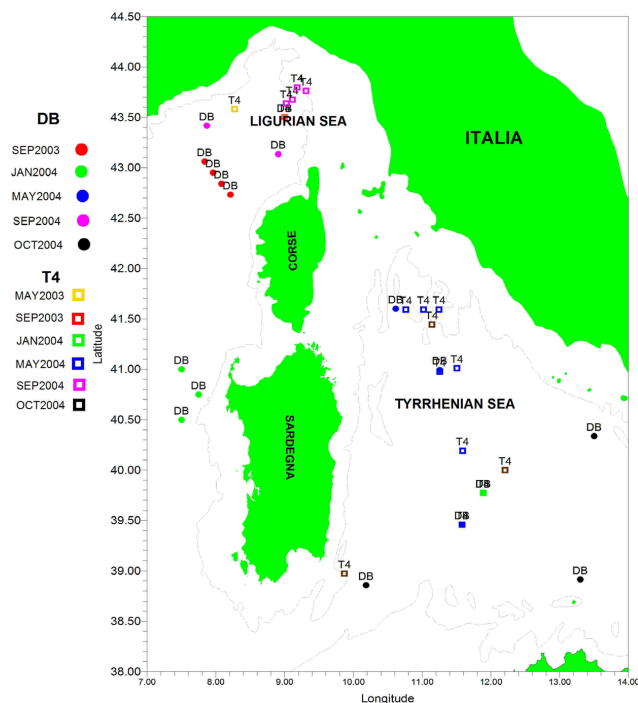


Fig. 1. The position of 55 XBT probes launched close to the corresponding CTD cast is shown: the mean difference was 0.0002° both in latitude and in longitude, with a time delay ranging from 60 up to 480 s (the mean value was 180 s). The averaged delay time was 180 s (ranging from 60 up to 480 s). The usual height of the launching position was 2.5 m a.s.l., with the exception of five T4 and six DB probes dropped from 8 m a.s.l. (superimposed symbols).

3 Data analysis

3.1 Extended use below the nominal terminal depth and acquisition time

Since April 2003, data acquisition beyond the nominal terminal depth has been the standard procedure for XBT probes dropped within MFS-TEP and ADRICOSM. In such a way, most of the copper wire on the probe side is used, and temperature values are recorded at depths greater than nominal. Practically, the depth in the Sippican software is set to 600 m for T4/T6 probes, to 900 or 1000 m for T7/DB probes, and to 2500 m for T5 probes. The Sippican MK-12 Electronic Help admits such a procedure, but a terminal depth increased by no more than 20% is recommended.

The data acquisition has been estimated as “valid” until sharp variations toward negative values are recorded (usually -2.5°C), indicating that the copper wire breaks on shipside, or high values are detected (about 36°C), implying a wire break on probe-side.

The comparison between XBT and contemporaneous and co-located CTD profiles does not show unusual features in the recorded values. T4 probes have measured tempera-

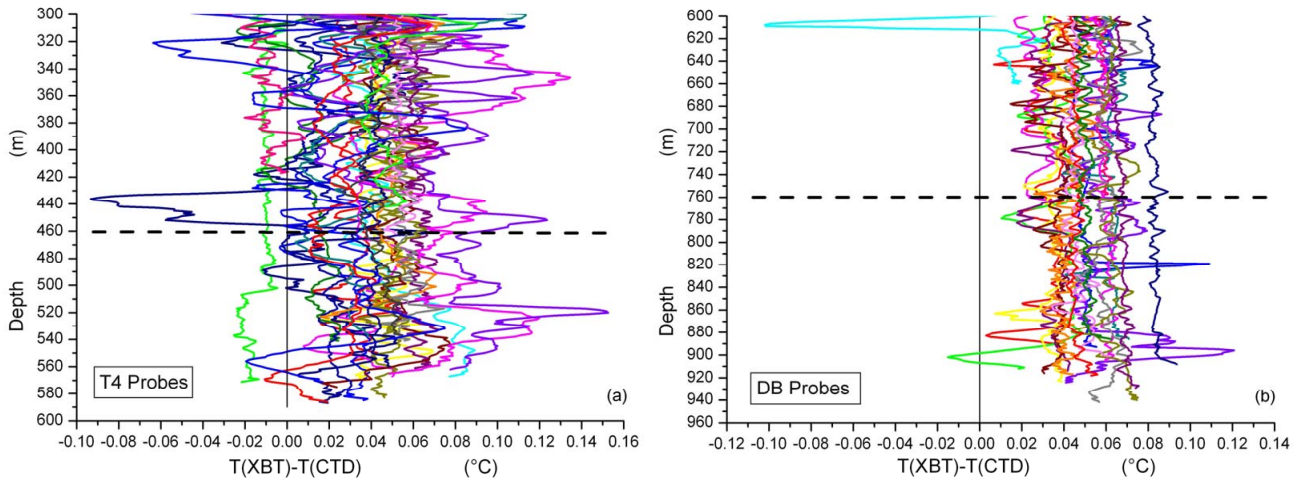


Fig. 2. Temperature difference ($T(\text{XBT})-T(\text{CTD})$) in deeper part of each XBT profiles: in (a) for 28 T4 probes below 300 m depth, in (b) for 27 DB probes below 600 m depth. The depth is computed by using IGOSS coefficients and data processing described in Manzella et al. (2003). The black dashed line indicates the nominal terminal depth. The plots have different scales.

tures higher than the corresponding CTD (Fig. 2a): only one profile always has values consistently lower, and four profiles have significant spikes corresponding to thermal structures. The range of temperature differences below the nominal terminal depth is $-0.03^{\circ}\text{C} \leq \Delta T \leq +0.16^{\circ}\text{C}$. On the other hand, DB probes have always recorded temperatures higher than the corresponding CTD, and four profiles show evident spikes (Fig. 2b); their range of variability below their nominal terminal depth is $-0.02^{\circ}\text{C} \leq \Delta T \leq +0.12^{\circ}\text{C}$.

The depth of a probe at a selected time is estimated through a fall rate equation, but the true free parameter is the acquisition time (AT), the temperature values being recorded at a fixed rate. The maximum value of the acquisition time depends on the XBT type: it is calculated by dividing the number of rows in the acquisition file by the sampling rate of 10 Hz. In Table 1, AT values corresponding to the nominal terminal depth are shown. AT values lower than the nominal one (mainly due to spikes or failed launches) were not included in the statistics, as well as in the case of profiles without a signal clearly indicating that acquisition was stopped. Several probes dropped in extended mode within MFS-TEP and ADRI-COSM projects continued their data acquisition up to the selected end, even after the probe touched the bottom. If a XBT probe is dropped from a steady vessel, its AT values can be assumed to be nearly coincident with the maximum value (e.g. about 90 s for T4/T6, and 150 s for T7/DB probes). Analyses of XBT probes launched within MFS-TEP and ADRI-COSM confirm that such values are more or less constant when the ship speed v is smaller than 19 kn for T4 and smaller than 16 kn for DB probes, and, as expected, they decrease at higher speed (Table 1). As an example, the frequency distribution of the acquisition time values is shown

in Fig. 3a for T4 probes, and in Fig. 3b for DB probes. In this case, the distribution is practically Gaussian around the experimental mean value.

For XBT probes dropped from ships moving faster than the maximum value indicated by the manufacturer, AT values smaller than the nominal ones should be expected, and experimental results agree with this assumption. The mean AT values for 191 DB probes launched from May 2004 to December 2005 along the transect Genova-Palermo from ships moving at speed $v > 20$ kn are detailed in Table 1. Temperature values recorded by DB probes do not show evident anomalies depending on the ship speed.

The dataset of T7 probes within MFS-TEP and ADRI-COSM is small: 68 probes were launched from ships moving at $v \leq 15$ kn, and 15 probes from ships moving at $v \sim 17$ kn. Their AT values are as great as the ones of DB probes (Table 1).

Only 14 T5 probes were dropped with extended acquisition: as for the other XBT types, their AT values are about 20% higher than the nominal one (Table 1).

3.2 Factors influencing the XBT motion

3.2.1 Launching position height

The acquisition of good data in the near surface layer is strongly dependent on events occurring during the first seconds after the probe touches seawater: therefore, the launching procedures (including the height (H) of the launching point above the sea level, and the verticality of the probe when it goes into the seawater), are briefly analysed. In the working procedures, it is fundamental to make sure that the probe quickly reaches a spin rate of about 15 Hz in seawater,

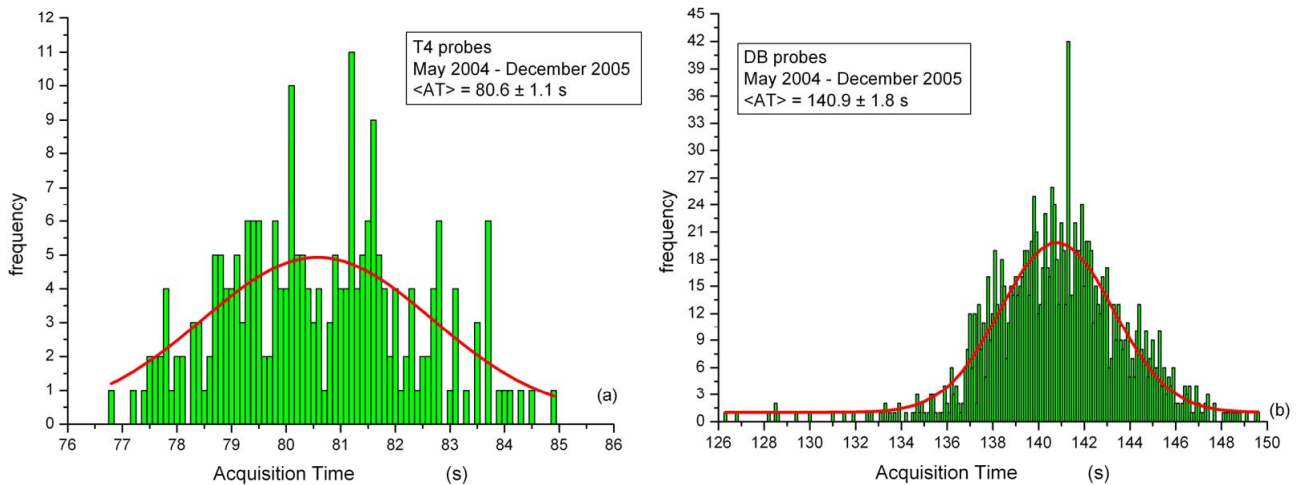


Fig. 3. Frequency distribution of acquisition time (AT) for different type of probes. In (a), values for T4 probes launched within MFS-TEP along the transect Genova-Palermo from May 2004 to December 2005, at a ship speed ranging from 21 to 27 kn, are shown. In (b), values for DB probes dropped in the same period at $v \leq 20$ kn. Some counts at AT=141.3 s are due to probes dropped by setting the terminal depth to 900 m in software.

a value needed to maintain the vertical direction of the motion through the water and the standard falling conditions. Analyses performed by Hallock and Teague (1992) showed that T4/T6/T7/DB probes require more or less 1.5 s to reach a falling speed of about 6.5 ms^{-1} , independent of the entry speed.

The manufacturer recommends $H \sim 2.5$ m a.s.l.: if external causes do not modify the fall, the entry speed when the probe touches seawater is about 6.5 ms^{-1} , as great as the A coefficient in the fall rate equation. A much higher launching height increases the entry speed, and the depth computed by software could be wrong. It is also important that the probes touch the seawater in the vertical position, otherwise the initial falling velocity within seawater could be smaller than 6.5 ms^{-1} . In this case, the actual XBT depth would be smaller than the one computed by software. The number of slant impacts could increase when the ship moves faster or the wind is stronger, but the evaluation of what really happens is unpredictable. Usually, the depth discrepancy can be identified in the region where a thermal gradient starts. Non-standard launching conditions should be described by an offset term (smaller than 5 m) added to the depth computed by applying the usual fall rate equation. Before the analyses made by Hanawa et al. (1994, 1995), this was the solution proposed in some papers in order to calculate better the XBT depth (i.e. Singer, 1990).

Differences between the theoretical (i.e. computed by using the fall rate equation), and the real estimated depths D ($\Delta D = D(\text{estim}) - D(\text{theor})$) were obtained by Green (1984), who analysed the influence of the launching position height (i.e. the entry speed). He found depth values greater than the nominal ones: his correction varies from $\Delta D \sim 1.1$ m (if $H \sim 8.5$ m) to $\Delta D \sim 1.9$ m (if $H \sim 20$ m).

In September–October 2004, twin XBT drops were made during the same CTD cast from different positions ($H \sim 2.5$ m and $H \sim 8.0$ m, respectively), aiming to check the influence of the launching position height, namely the depth difference predicted by Green (1984). The strong seasonal thermocline has offered a good reference feature for the test; in addition, the launching conditions have been optimal: ship motionless, good weather and sea status. The time delay between the pair of drops and the CTD cast was smaller than 480 s, i.e. the variation of the depth of upper thermocline should have been very small. In all twin T4 profiles, such thermal structure is generally well reproduced both in depth and in intensity, independent of the time-delay and the height of the launching position (see Fig. 4, where the temperature gradient profiles are shown). Sometimes, discrepancies appear below this region (observed depths greater than CTD values), indicating some variation in the probe motion (Fig. 4d).

Results are significantly different for DB probes: in general, their profiles reproduce well the intensity of the upper thermal gradient, but not the depth. Only one pair of DB twin drops has both profiles fitting the CTD profile in an excellent way (Fig. 5e). In four cases (Figs. 5a, b, c, and f), the last dropped probe overestimates the depth of the maximum gradient value, whereas only one probe (Fig. 5d) underestimates such a value. In general, the first dropped probe has a smaller discrepancy, with only one significant difference (Fig. 5c).

When the height of launching position is considered, the probes dropped at $H \sim 8$ m a.s.l. fit well the depth of maximum gradient in three cases (Figs. 5a, b, and e); in two cases, the XBT profiles underestimate the true depth (Figs. 5c and d), whereas the only case with an overestimated depth is shown in Fig. 5f. In a certain way, results for DB probes dropped at $H \sim 2.5$ m (as recommended by the manufacturer)

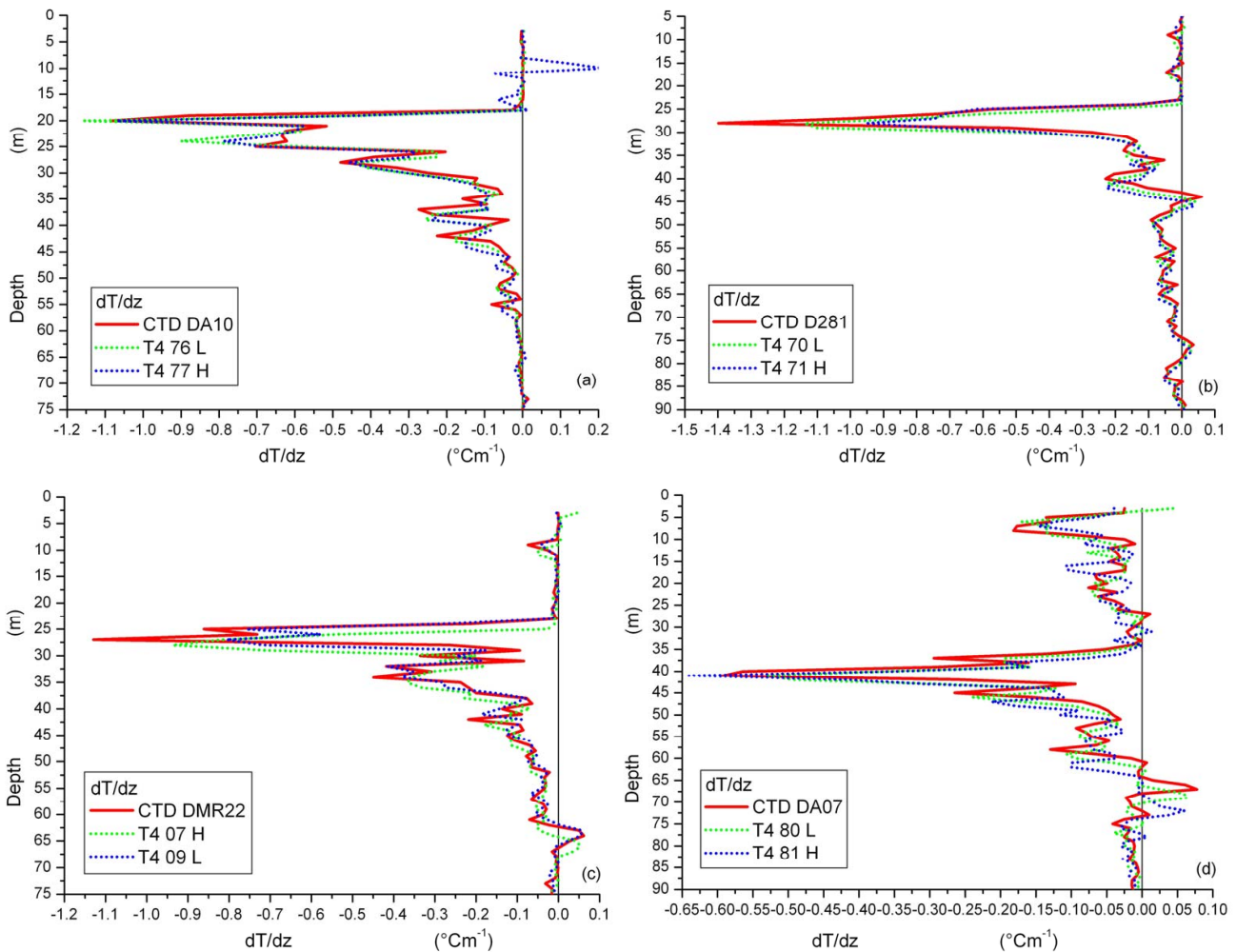


Fig. 4. Thermal gradient profiles in near surface layer for four pairs of twin T4 drops: the green short dotted line always represents the former dropped probe, the blue short dotted line the latter one. The plots have different scales.

are astonishing: in four cases (Figs. 5a, b, c, and d), the depth of the maximum gradient value is overestimated, whereas only two profiles (Figs. 5e and f) have the right depth.

The dataset of twin drops has poor statistics, and the results of the test are uncertain: the starting depth of the upper thermal gradient measured by XBT probes is either deeper or shallower than the true depth, without apparent correlation with the launching position height and time delay. Therefore, further tests are required in order to obtain an answer to such a problem.

3.2.2 XBT probe mass

The mass of a probe is a parameter potentially influencing its motion, and small manufacturing differences (i.e. in wire length) make any probe different from another (Thadathil et al., 1998). The manufacturer states that the weight of XBT probes of the same type should vary within a range of few

grams. As remarked by Hanawa and Yoshikawa (1991), XBT probes made in different periods have small and random changes in shape and weight due to the wire technical coating process by enamel. A wire thicker than normal has less enamel: therefore, the linear density is higher and the buoyancy of the probe is reduced. Consequently, the starting fall-speed is higher, but its weight reduction is faster because of the unreeling process of heavier wire.

Following Seaver and Kuleshov (1982), a weight variability of 0.36% induces a depth difference $|\Delta D| \geq 1.6$ m at 750 m depth (the standard deviation is 1.1 m). The inclusion of the effect of air entrapped in the probe induces weight variability up to 2%, with $|\Delta D| \sim 8.8$ m at 750 m depth. The nose roughness, whose variability is due to the practical impossibility to have a micrometric precision in the shape of the nose, introduces further depth variability at a level of $|\Delta D| \sim 7$ m at 700 m depth (Table 3).

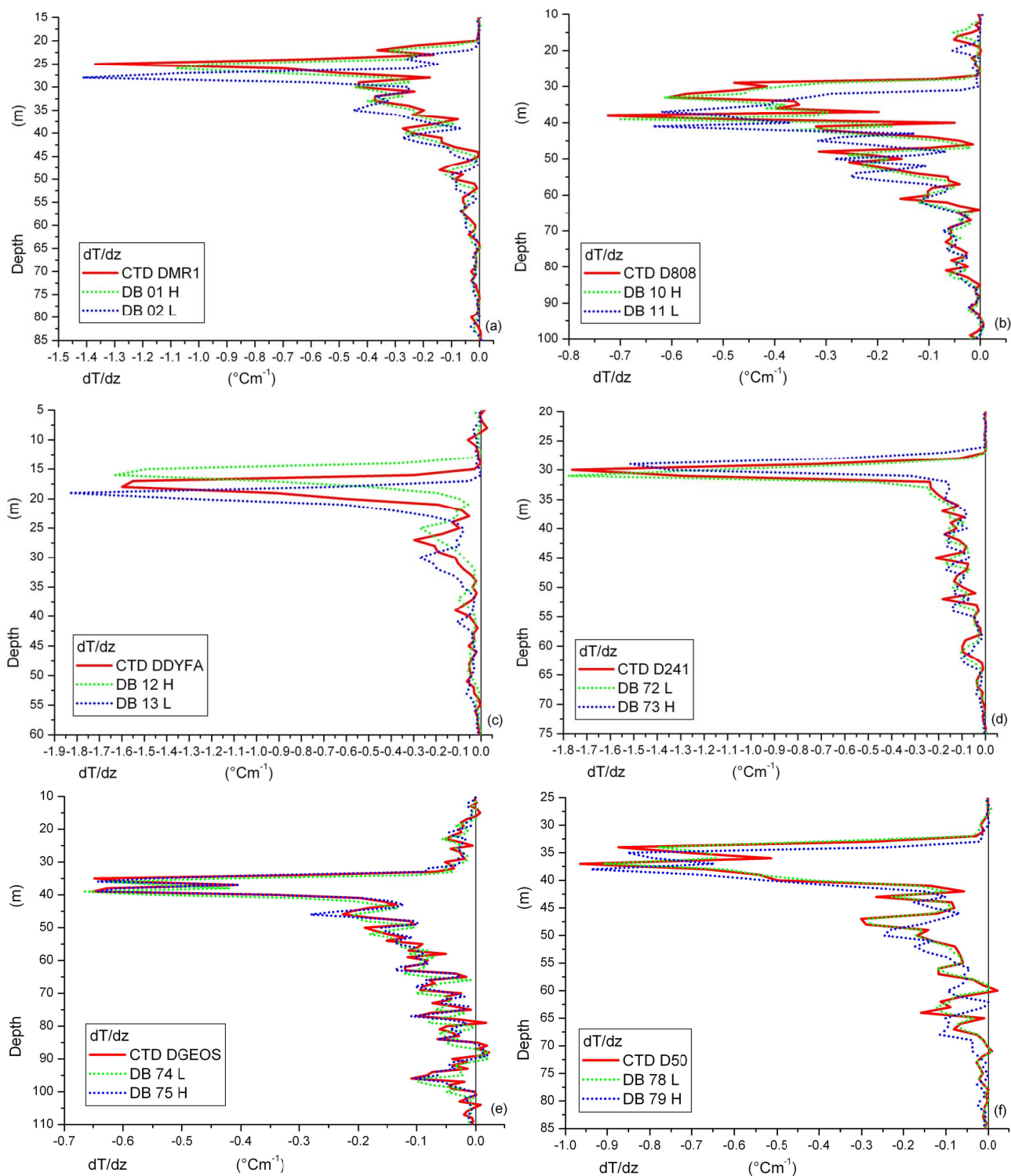


Fig. 5. As in Fig. 4, for all the pairs of twin DB drops. The plots have different scales.

Table 3. Effects induced on the values of fall rate coefficients and computed depth quoted by different authors for T7/DB probes (see the text for details). Depth values quoted in (*) are from Seaver and Kuleshov (1982).

Source of Uncertainty	Depth m	Variation on A (ms^{-1})	Variation on B (ms^{-2})
Horizontal Current $v=0.25 \text{ ms}^{-1}$	-0.7	-0.005	-0.00003
Weight variability*	± 8.8	± 0.013	± 0.00007
Nose roughness*	± 7.0	± 0.063	± 0.00055

In order to identify a possible correlation between weight and acquisition time, the mass (in air) of some boxes of DB probes was measured. In detail, each probe within the canister (but without the cap) was weighed before the drop, and the components of the canister were again weighed after the launch. In addition, the components of some probes were weighed, and the length of their copper wire was measured. When different boxes are compared, the mean weight of the whole probe and plastic canister (averaged on 12 probes) is more or less constant, with the standard deviation (4 g), but the probe-to-probe variability within a box is high (up to 15 g, about 1.5% of the weight). The range of variability of retaining pin and shipboard plastic spool is small, but large for the plastic canister, probably due to the quantity and characteristics of the insulating wax. From the comparison of the weight of the components, the range of weight variability of the naked probes is 5 g (more or less as the manufacturer states), but any estimate of its influence on the motion in seawater (mainly on the fall rate coefficients) is impossible. The weight of the zinc nose is constant for both T4 and DB XBT types, within 1 g variability. Therefore, 4 g is the more probable weight variability for the plastic and the wire component of a probe. The measured linear density of copper wire varies between 0.116 and 0.121 gm^{-1} , independent of the XBT type, or, in other words, one gram of wire corresponds to about 8.5 m. This means that the variability due to the uncertainty in the probe weight is up to about 35 m (or more than 5 s in acquisition time).

3.2.3 Other sources of uncertainties

A constant horizontal current having $v=0.25 \text{ ms}^{-1}$ has been considered from the theoretical point of view: it can shift the probe from the vertical fall up to 22 m for T4/T6 probe (at 550 m depth), and to 35 m for DB (at 900 m depth). Consequently, the real depth is smaller than the computed one. The estimated effect of such terms on fall rate coefficients for DB probes is reviewed in Table 3.

3.3 Start-up transient

The time response of the recording system can influence the quality of XBT measurements mainly in upper layers, where quick thermal changes occur. The thermistor has a time con-

stant (TC) of 0.15 s: this is the time required to detect the 63% of a step thermal signal, whereas the overall time constant (OTC), which describes the response time of the whole acquisition system, is slightly greater (OTC \sim 0.16 s). During such a time interval, the probe falls about 1 m and this is the depth uncertainty intrinsic to the acquisition system. The bridge circuit reaches equilibrium within two sampling intervals (the thermistor output is sampled at a constant rate of 10 Hz), but an interval as great as 4.5 TC (about 0.6–0.7 s) might be needed before the probe completely detects a temperature variation. In addition, the probe nose and the read-out card might influence the initial transient time up to about 0.1 s (Roemmich and Cornuelle, 1987). Consequently, it seems realistic to suppose that the true water temperature in near surface layers can be detected below about 4 m depth (or 0.5 s in acquisition time). It has to be pointed out that Stegen et al. (1975) eliminated values from the surface down to 4 m depth, Kizu and Hanawa (2002a) proposed a cut varying from 2 to 10 m, depending on the readout card, whereas Manzella et al. (2003) excluded temperature values from surface down to 5 m.

In this work, the first ten recorded temperature values of all the available profiles have been analysed in order to calculate the Empirical Time Constant (ETC), which is defined as the time needed before the probes reach the stationary regime in seawater. It is identified by the occurrence of three consecutive temperature values differing less than 0.10°C (the nominal accuracy) within the first ten measurements. The mean value of such time intervals for all the probes of a selected type is the mean response time (ETC) for that XBT type. The value obtained for both T4 and DB probes is ETC=0.3 \pm 0.1 s (twice the overall time constant of the acquisition system). Then, the sequence of temperature values of each XBT profile has been modified by eliminating the values recorded up to time t =ETC, and the measurement at the time t =ETC+0.1 s has been considered as the first one. The first three temperature values have been eliminated from each XBT profile, and the fourth recorded value is the first valid value. This implies a 2 m correction to the whole profile.

After the application of this procedure, the discrepancies between XBT and CTD temperature values in upper layers are significantly reduced (Fig. 6a for T4 and Fig. 6b for DB probes). The mean temperature difference profile is more

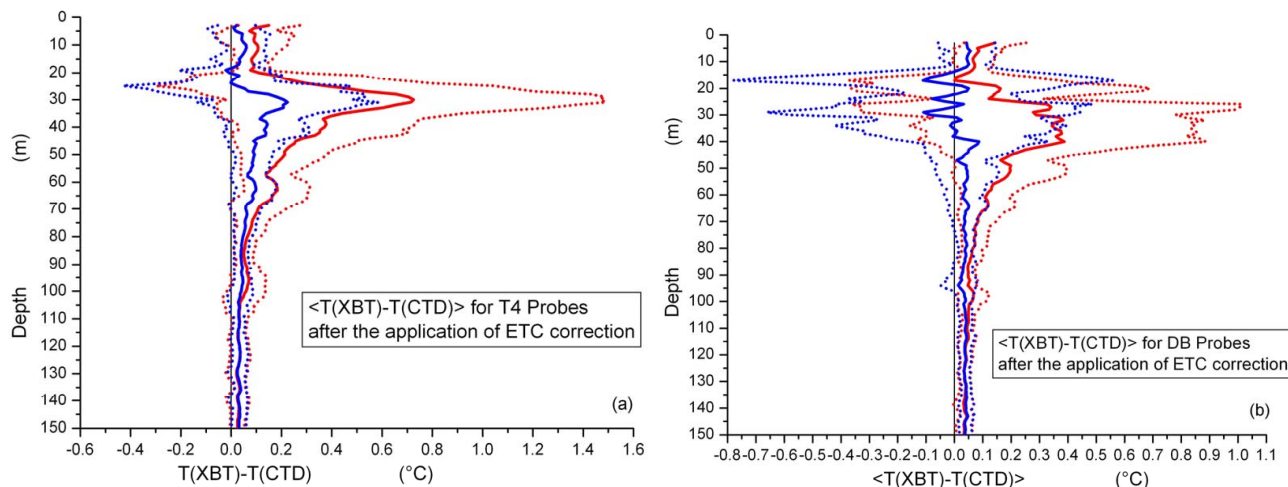


Fig. 6. Comparison between mean temperature difference (with one standard deviation) with data processing as in Manzella et al. (2003), in red, and after the application of ETC correction, in blue: in (a) T4 probes, and in (b) DB probes. The plots have different scales.

symmetric with respect to the null value, and the initial position of thermal structures in upper regions is reproduced better for both XBT types. In any case, this empirical procedure does not provide any understanding of phenomena related to the correction.

3.4 Calibration of XBT probes and data acquisition system

Several authors have detected discrepancies between the XBT values and selected reference temperatures either in situ (Heinmiller et al., 1983) or in a calibration bath: always $T(\text{XBT}) \geq T(\text{CTD})$. Since the early 80's, it has been suggested that the calibration of XBT probes could provide indications of the source of errors (Georgi et al., 1980), and the variability in temperature differences has been attributed to the probe-to-probe variability, e.g. Georgi et al. (1979, 1980), Roemmich and Cornuelle (1987), and Budéus and Krause (1993).

Seaver and Kuleshov (1982) found a difference of 0.025°C (0.015°C in a controlled and digitised interface), which was ascribed to temperature-resistance characteristics of the thermistor. Such a temperature difference is equivalent to a depth error varying from a few metres (in the upper warm layer) up to 20 m (at the bottom). Roemmich and Cornuelle (1987) measured a difference of $0.02\text{--}0.03^\circ\text{C}$, and identified a small pressure effect on the thermistor (about $0.01^\circ\text{C}/1000\text{ m}$) due to the non-standard quality of the production of the probe components.

In the middle of the 90's, several hundreds of T4 and T7 probes were calibrated at NURC Laboratories. The selected reference temperatures were $T=12^\circ\text{C}$, and $T=22^\circ\text{C}$: systematically, XBTs indicated temperatures higher than the

bath (Zanasca, 1996²; private communication, 2005). For T4 probes, the overall difference was $0.02 \pm 0.02^\circ\text{C}$ at the lower temperature and $0.03 \pm 0.03^\circ\text{C}$ at the higher one, whereas T7 probes showed a constant difference ($0.02 \pm 0.04^\circ\text{C}$). The use of various PCs and readout cards (of the same type) can also influence the results of measurements. When two different data acquisition systems were connected with the same XBT probe, a difference of $0.02 \pm 0.01^\circ\text{C}$ was measured (Zanasca, 1996²), whereas Kizu and Hanawa (2002b) obtained a much greater effect (up to 0.10°C), depending on the type of recording card.

In September 2004, six T4 and six DB probes were calibrated at NURC Laboratories at four reference temperatures (12.5 , 16 , 20 , and 24°C). The data were recorded by always using the same acquisition system composed by a PC, Sipican MK-12 card, cable, and connection box. Each probe was immersed in the bath 10 min before the data acquisition, which was 30.0 s long. Such a procedure should allow the identification of the intrinsic bias due to the thermistor and the data acquisition system. For each probe the measured temperatures are always higher than the bath and increasing with the temperature (from 0.04°C to 0.08°C), the standard deviation being 0.01°C at the lower temperature, and 0.03°C at higher values (Fig. 7a for T4 and Fig. 7b for DB probes). When compared with earlier calibrations made at NURC, new results indicate higher temperature differences, but the standard deviation is smaller. On the other hand, similar temperature differences were confirmed by in situ measurements (MEDARGO floats), although most of them were not exactly contemporaneous and co-located with XBT probes dropped during MFS-TEP (Poulain, private communication, 2005).

²Zanasca, P.: NURC Internal Notes (unpublished), 1996.

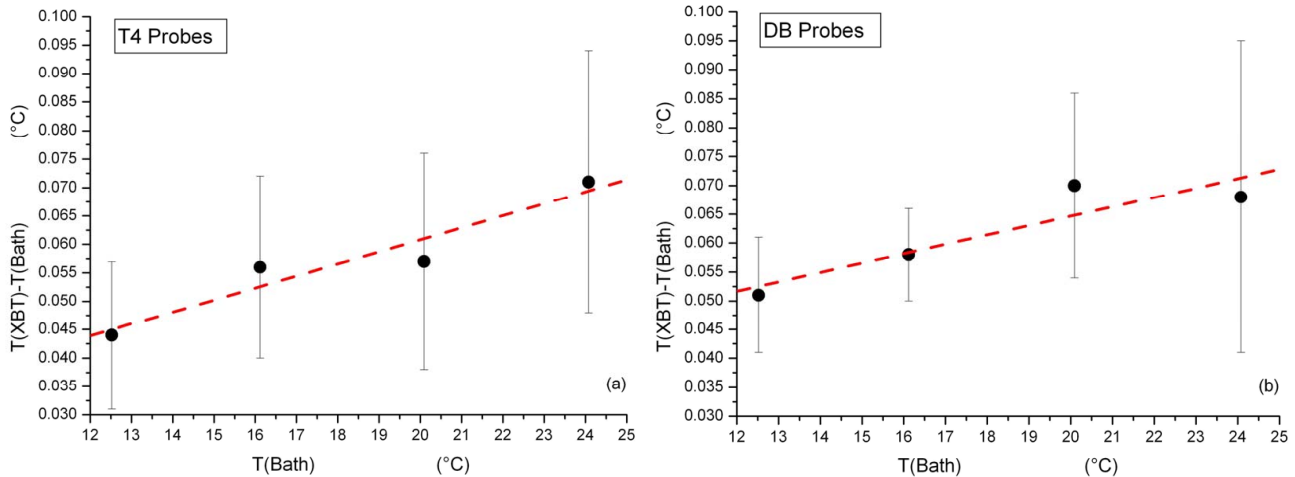


Fig. 7. The mean values of temperature differences at each reference point (and the standard deviation) from calibration: in (a) for T4 probes, in (b) for DB probes.

A linear function of temperature, $\Delta T(T) = q + a * T$, reproduces well the temperature differences measured in this calibration (Figs. 7a and b): the difference changes linearly with the temperature. The best-fit values are:

- T4: $\Delta T(T) = (-0.01845 \pm 0.00852)^\circ\text{C} + (-0.00212 \pm 0.00046) * T$;
- DB: $\Delta T(T) = (-0.03222 \pm 0.00970)^\circ\text{C} + (-0.00162 \pm 0.00052) * T$.

The second coefficient depends on the wire length, which is about 1800 m for T4 (550 m in the probe and 1250 m in the canister) and about 2300 m for DB (950 m and 1350 m), and on the characteristics of the thermistor, but it is hard to evaluate each specific contribution. The value of the second coefficient for DB probes should be smaller than the one for T4 probes, because of the increasing influence with the temperature of the wire length term with respect to the thermistor term. The obtained values seem to confirm such an interpretation.

When calibration starts soon after the insertion of probes (having initial room temperature) in the bath, a significant difference (up to 0.5–0.7°C) has been observed in the first part of the recorded profiles. Only after a time interval as large as 50–70 s, but linearly depending on the difference between room and bath temperature, the temperature discrepancy decreases at the previously quoted values. It is sufficient to put the probes in the bath before the measurements for a time interval ranging from 30 to 60 s to eliminate such a difference.

3.5 Data processing procedures

The quality control procedures detailed in Manzella et al. (2003) were designed for the characteristics of Mediterranean waters.

They involve several steps:

- Initial visual inspection of the profile with a gross range and position control. The distance and time interval between two drops are calculated, and the corresponding velocity derived and compared with the maximum ship speed;
- Elimination of spikes, which are identified by computing a median value in a 3.5 m interval and comparing this with the original profile value. The substitution is applied if the difference between the value and the median is greater than an established tolerance (the selected value is 0.1°C, the nominal accuracy of the probe). The window interval used to calculate the median and the tolerance are defined as external parameters;
- Re-sampling at 1-m interval by means of a polynomial fit. Then, a smoothing is done with a Gaussian filter with 4-m e-folding depth, the minimum value that allows full elimination of the high frequency noise in the terminal part of the profile;
- General malfunction control that involves checking if the temperature gradient between adjacent data is greater than a certain parametric value. A message warns the operator.
- Comparison with climatology, in terms of “distance” of the XBT data from the mean monthly profile (good if less than 2 standard deviations);
- Final visual check, confirming the validity of profiles and providing an overall consistency.

The above procedure has been modified in order to reduce the disagreement between raw and processed XBT profiles, and

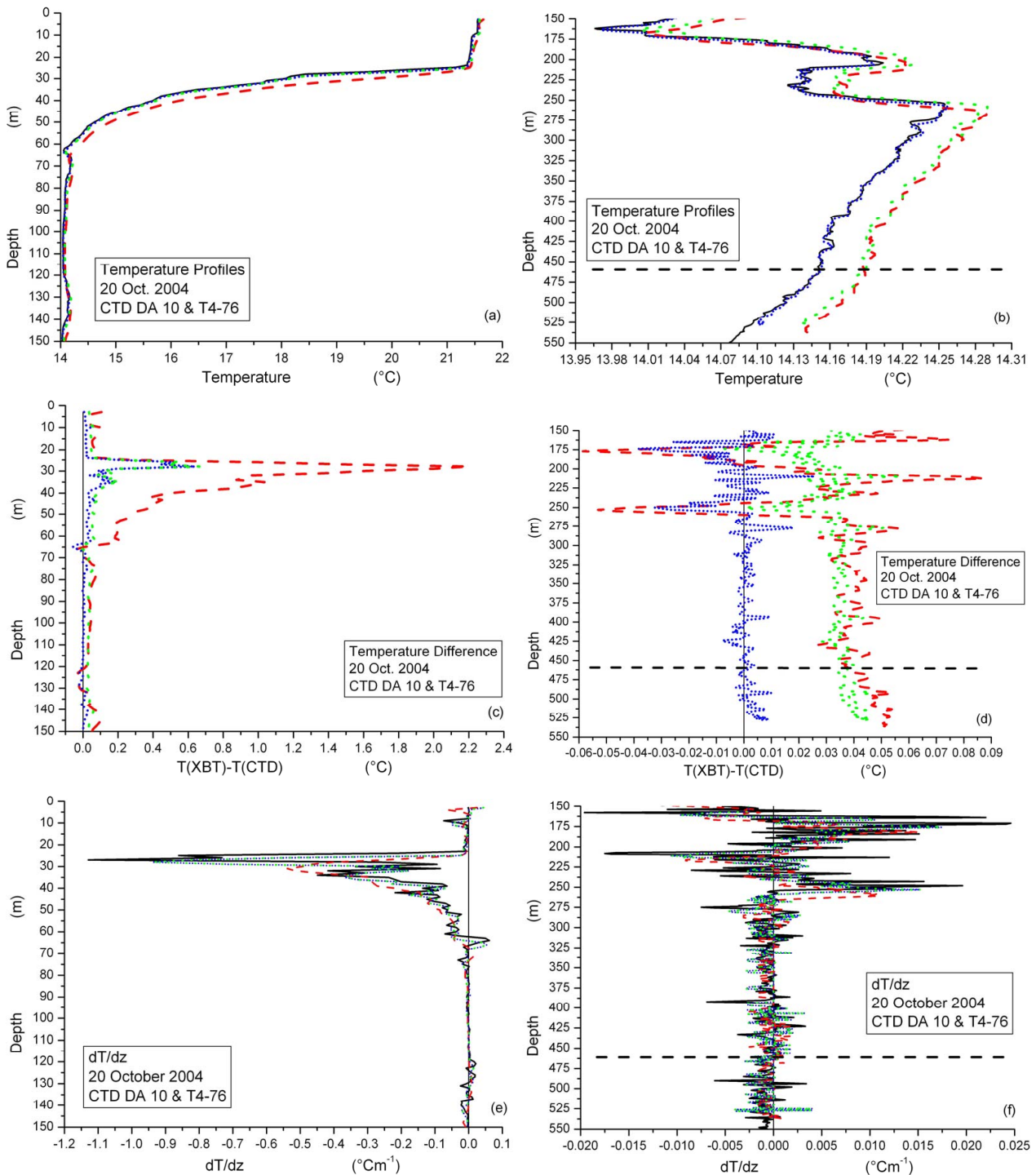


Fig. 8. Profiles of different thermal characteristics of a T4 probe and of the correspondent CTD cast: on the left column the range is 0–150 m depth, on the right column the values below 150 m are plotted. In (a) and (b) the temperatures are shown: CTD (full black line), XBT with old data processing and IGOSS coefficients (dashed red line), XBT with new data processing and new fall rate coefficients (dotted green line), XBT with new data processing, new fall rate coefficients and temperature correction (short dotted blue line). In (c) and (d), the difference $T(\text{XBT}) - T(\text{CTD})$ is plotted: XBT with old data processing and IGOSS coefficients (dashed red line), XBT with new data processing and new fall rate coefficients without temperature correction (dotted green line), XBT with new data processing, new fall rate coefficients and temperature correction (short dotted blue line). In (e) and (f), dT/dz values are shown, where the lines and the colours are the same as in (a) and (b). The plots have different scales and units.

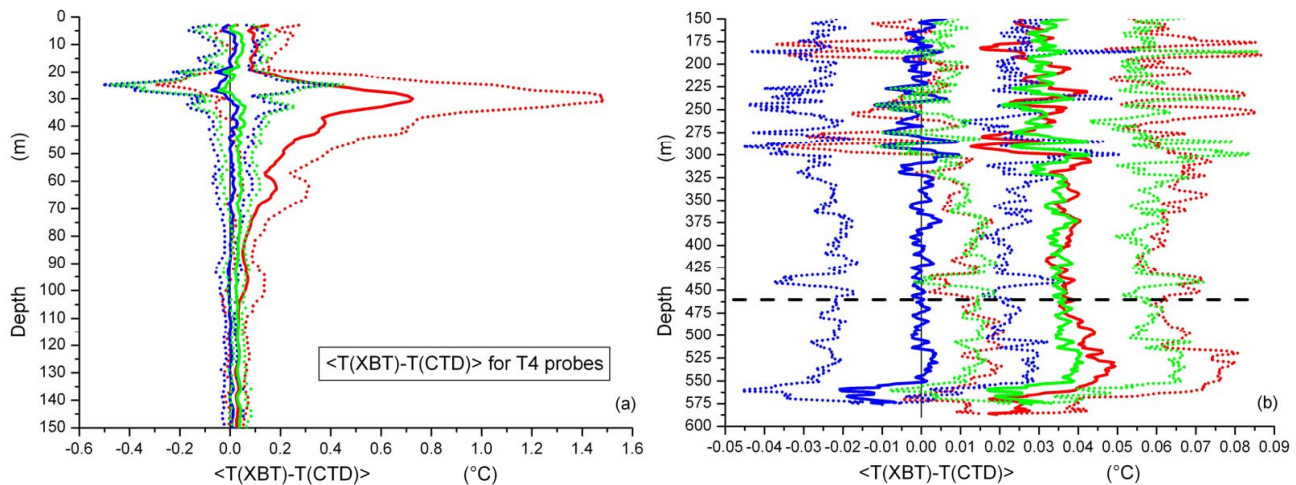


Fig. 9. Mean temperature differences (full line) with one standard deviation (short dotted lines) for T4 (and T6) probes (28 profiles). The used data processing are: IGOSS fall rate coefficients and procedures as in Manzella et al. (2003) (red); new T4 fall rate coefficients and new procedures without temperature correction (green), and with temperature correction quoted in Table 5 (blue). In (a) the upper region is shown, whereas the bottom is plotted in (b); the nominal terminal depth is added (dashed black line).

CTD profiles. The time sequence has a uniform increment, due to the 10 Hz sampling rate: therefore, the Gaussian filter has been applied to each raw profile before de-spiking and 1-m reduction, but in three contiguous time intervals, which are identified by the start and the end of the seasonal thermocline. In the upper (from the surface down to the start of the thermocline) and the intermediate (down to the base of thermocline) regions, the selected e-folding time interval is 0.1 s (less than 1 m in depth), whereas the selected value is 0.7 s (about 4 m) in the deeper region (from the base of the thermocline down to the bottom). When the thermocline is absent, the value 0.7 s is valid for the whole profile. Software identifies the seasonal thermocline (if any) by searching for a point where for four consecutive times the temperature difference between two consecutive measurements is lower than -0.10°C . In a similar way, the base of the thermocline is defined where for four consecutive times the temperature difference is greater than -0.10°C . After this, the de-spiking procedure and the transformation of the temporal sequence of temperature values in the depth sequence (step 1 m) are applied, as described in Manzella et al. (2003). Then, temperature values from surface down to 3 m depth and the last three values of each XBT profile are eliminated, whereas in Manzella et al. (2003) the first accepted value is at 5 m depth, and the last five values are excluded from quality-controlled profiles.

The small window of the Gaussian filter, that is applied before the de-spiking procedure, does not eliminate spikes. Conversely, this procedure allows a better agreement between CTD and XBT profiles (mainly where the temperature strongly varies), and in the dT/dz profile (Figs. 8e and f).

3.6 New fall rate coefficients

From the analysis of temperature profiles, it appeared that the IGOSS coefficients (Table 2) do not correctly calculate the depth of the thermal structures in Western Mediterranean seawaters, both at deeper depth (Figs. 8b and d), and in correspondence with the upper thermal gradient (Figs. 8a and c).

In such a region, the XBT calculated depth is usually greater than the value indicated by the CTD. It is realistic to suppose that the discrepancy in the near surface layer cannot be ascribed to the fall rate coefficients: their variation produces insignificant depth difference in the upper region. On the other hand, new coefficients should provide a good solution improving the agreement at greater depth.

The profiles of mean temperature difference processed either with IGOSS coefficients and quality control procedures as in Manzella et al. (2003), or with the proposed technique, are shown in Figs. 9 and 10. The use of the new procedures detailed in Sects. 3.3 and 3.5 significantly reduces the disagreement in the upper layers for T4 probes (Fig. 9a), whereas DB probes have an even stronger variability in the near surface region (Fig. 10a), as well as in the region between 200 and 300 m depth (Fig. 10b). On the contrary, below this depth, the range of variability of DB probes is smaller. In any case, the observed variability below the nominal maximum depth is probably due to the poor number of samples at depths greater than about 550 m for T4 (Fig. 9b), and about 920 m for DBs (Fig. 10b). The difference of the depth of the thermal structures increases toward the bottom, especially for T4 probes: therefore, new fall rates coefficients seem to be required. The Mediterranean Sea needs

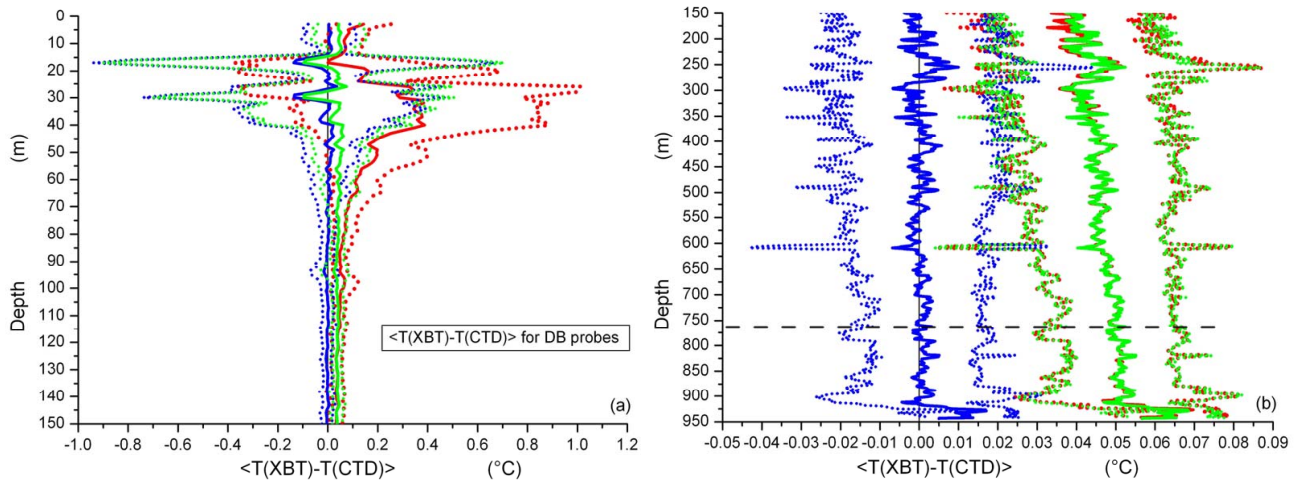


Fig. 10. As in Fig. 9, for DB probes (27 profiles). The plots have different scales.

customized coefficients: local seawater characteristics could induce different values of the falling speed because of viscosity variations (Hanawa et al., 1995), although Thadathil et al. (1998) excluded any influence of temperature on fall rate coefficients in the Indian Ocean, where their analysis was carried out.

The water temperature in the Mediterranean Sea is higher than 12.5°C, independent of depth, latitude and season, instead of the values decreasing down to few degrees in the World Oceans. In addition, the temperature profiles are not a decreasing monotonic function of depth. In general, higher temperature implies lower viscosity: consequently, a motion with higher speed is expected, whereas higher salinity acts in the opposite direction both on density and on viscosity, but its influence is much smaller. The salinity in Mediterranean Sea is within the range $36.00 \leq S \leq 39.40$ PSU, to be compared with the values of the dataset analysed in the IGOSS Report ($34.00 \leq S \leq 37.00$ PSU).

Unfortunately, the technique proposed in Hanawa et al. (1994, 1995) cannot be applied to the temperature profiles from the Mediterranean Sea because of the high vertical homogeneity that frequently occurs. In fact, that method can sometimes fail “...to detect depth-differences when the temperature gradient is constant in a section of the profile, or when the XBT temperature profile has features not matched by the CTD profile” (Hanawa et al., 1995). For example, the CTD values of dT/dz below 250 m depth are always smaller than $0.005^\circ\text{C m}^{-1}$ (Fig. 8e), whereas the T4 probe shows even smaller values, and its final part has null value, due to constant recorded temperatures. New fall rate coefficients, reproducing better the depth of the thermal structures identified by the CTD profile, have been searched for in the following way: (71 × 13) profiles for each T4/T6 probe, and (51 × 13) profiles for each DB probe have been computed by

varying the values of fall rate coefficients within the following intervals:

$$\begin{aligned} -T4 &: 6.400 \leq A \leq 6.750 \text{ ms}^{-1}, \quad 0.00180 \leq B \leq 0.00240 \text{ ms}^{-2}; \\ -DB &: 6.600 \leq A \leq 6.850 \text{ ms}^{-1}, \quad 0.00200 \leq B \leq 0.00260 \text{ ms}^{-2}. \end{aligned}$$

For both the XBT types, the steps used were 0.005 ms^{-1} for the A coefficient and 0.00005 ms^{-2} for the B coefficient: variations smaller than the quoted steps do not modify the calculated depth. In this way, 1-m accuracy in depth calculation at the bottom is possible (this is the intrinsic accuracy on depth due to the overall time constant of the acquisition system).

For each CTD profile, six reference points below 100 m depth are identified by visual inspection in correspondence with thermal structures. Obviously, the depth of the selected points differs from profile to profile. For corresponding points, the difference between the depth measured by the CTD and the one on each computed XBT profile is calculated, and summed up. The minimum value of the sum of the depth differences indicates the best pair of coefficients for the analysed probe. For each XBT type, the final values of fall rate coefficients are obtained by calculating the mean value, weighted on the length of each profile, and the results are shown in Table 4 (for a comparison with IGOSS values see Table 2). The fall rate coefficients computed for T4 and DB probes are valid also for T6 and T7 probes, respectively.

3.7 Temperature correction

When the profiles of temperature difference were analysed after the application of new fall rate coefficients, an evident shift appeared, mainly at depths greater than 150 m (Fig. 9b for T4, and Fig. 10b for DB probes, green lines). A better agreement between XBT and CTD profiles was obtained

Table 4. The values of the coefficients of fall rate equation computed by using the new proposed technique. The values of coefficients and the standard error for both the XBT types are rounded to the nearest values used in calculation.

Type	A (ms^{-1})	B (ms^{-2})
T4	6.570 ± 0.070	0.00220 ± 0.00010
DB	6.720 ± 0.060	0.00235 ± 0.00010

Table 5. Coefficients of the linear function of the depth $\Delta T(D) = \Delta T_0 + m * D$ for the analysed dataset.

	ΔT_0 ($^{\circ}\text{C}$)	m ($^{\circ}\text{C m}^{-1}$)
T4	-0.029 ± 0.001	-0.000016 ± 0.000001
DB	-0.039 ± 0.001	-0.000014 ± 0.000001

by introducing a correction term derived from a linear regression (function of the depth D) of the temperature differences, $\Delta T(D) = \Delta T_0 + m * D$. The value of the coefficient m was calculated by using the mean temperature difference values below 100 m down to 900 m for DBs, and below 100 m down to 550 m for T4 probes (Table 5). The constant term ΔT_0 , which could be thought of as a bias, is compatible with the temperature difference deduced from the calibration (Figs. 7a and b), whereas the coefficient m has a value very close to the coefficient of pressure effect described in Roemmich and Cornuelle (1987). The proposed correction makes the temperature difference symmetric around the null value (Fig. 9b for T4 and Fig. 10b for DB probes, blue lines).

3.8 Results

The calculated fall rate coefficients represent a compromise among the available probes: consequently, some spikes remain in temperature difference profiles. New procedures require the exclusion of two meters in the initial part of the profile due to the application of ETC. In Fig. 11, the maximum observed depth difference is shown, and compared with the estimated error of depth obtained by using IGOSS coefficients. Below 300 m depth, new fall rate coefficients reduce by some metres the disagreement with respect to the real depth, and the new measured maximum depth error is within 10 m for T4 probes (at a depth slightly greater than 550 m), and within 16 m for DB probes (at 940 m depth). Below the nominal standard depth, DB probes have a percent error in depth smaller than T4 probes.

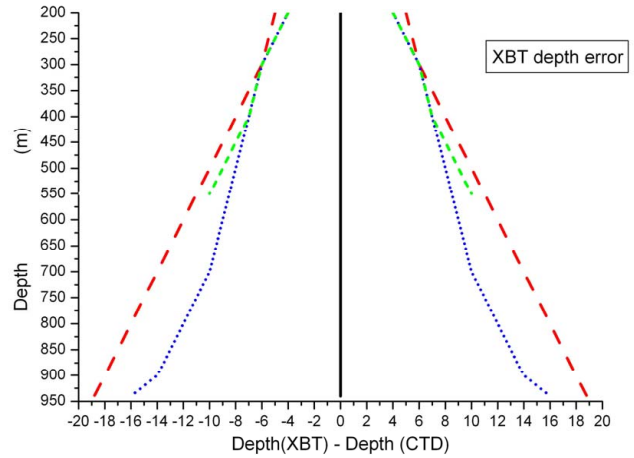


Fig. 11. The experimental maximum depth error for T4/T6 (green short dashed lines) and DB (blue short dotted lines). The depth of XBT probes is computed by using the data processing developed in the present work and new fall rate coefficients. The estimated depth error following Hanawa et al. (1994, 1995) is also quoted (red dashed lines), but their real maximum difference is little more than 20 m at about 550 m depth for T4 probes, and about 15 m for DB probes at about 920 m depth.

The calculated maximum depth of T4/T6 probes is always smaller than the depth computed by using IGOSS coefficients (the average depth difference is 10 ± 1 m), whereas DB probes have a less clear behaviour, but in general their depths are slightly greater (the average depth difference is 2 ± 1 m). When the best-fit pair of coefficients for each probe is used, the depth of each thermal structure on the XBT profile differs by no more than 3 m from the CTD value.

In Fig. 9 for T4 and in Fig. 10 for DB probes, respectively, the mean temperature differences obtained with different data processing and fall rate coefficients are compared. The main effect of the combined introduction of ETC, new data processing and new fall rate coefficients is a further reduction of the disagreement in upper regions (see Figs. 6a and b for a comparison), but significant discrepancies still remain (Figs. 9a and 10a, green lines). Some differences are also present at greater depth, usually in correspondence with thermal structures (Figs. 9b and 10b). It has to be pointed out that the range of temperature difference at greater depth for DB probes is smaller than that for T4 probes. In any case, temperature values recorded at depth greater than 550 m for T4 and 920 m for DB probes have to be carefully examined before use.

Finally, the temperature correction reduces the discrepancy between XBT and CTD profiles in both upper and lower layers (Figs. 9 and 10, blue lines), and makes the profile of the mean temperature difference practically symmetric around the null value.

4 Uncertainty in XBT measurements

The uncertainty (δT) in XBT temperature values is a very important parameter: the manufacturer indicates a constant value ($|\delta T| \sim 0.10^\circ\text{C}$), but the depth error has to be considered in order to calculate its true value. When the old quality control procedures and IGOSS fall rate coefficients are applied, the profiles of temperature differences between CTD and XBT show a dramatic rise of up to some degrees in the thermocline region (Figs. 9a and 10a, red lines). A drift of measurements toward warmer values is evident in the terminal part of the profiles (Figs. 2a and b). In the 300–600 m depth region, the range of measured temperature differences is $-0.10 \leq \Delta T \leq 0.16^\circ\text{C}$ for T4 probes and $-0.06 \leq \Delta T \leq 0.11^\circ\text{C}$ for DB probes; below this depth, but only for DB probes $-0.02 \leq \Delta T \leq 0.12^\circ\text{C}$. It is hard to give an estimate of the uncertainty, because of the asymmetry in the temperature difference: the value $|\delta T| \sim 0.10^\circ\text{C}$ is a realistic approximation only below the thermocline region.

The present analysis confirms that the temperature uncertainty is strictly related to the depth error and to the profile of temperature difference between CTD and XBT measurements. Depth errors (implying a significant temperature difference between profiles) still remain, despite the use of new fall rate coefficients and new data processing. It is the main source of the temperature uncertainty in the upper region and in correspondence with thermal structures at greater depth.

The main improvement to the new estimated uncertainty is due to the application of the ETC cut and of the temperature correction: the former in the region where the thermocline starts (Figs. 6a and b, blue lines), and the latter at greater depth (Figs. 9b and 10b, blue lines). Both terms make the profile of the temperature difference much more symmetric around the null value.

In practice, the cut of the first three recorded values strongly reduces, but does not fully eliminate, the depth difference where the upper thermocline starts, whereas the temperature correction excludes a bias term correlated with wire, thermistor, read-out card, and electronics of the data acquisition system. Such a term is more or less as great as the differences measured in the calibration, which indicates also a standard deviation within the range $|0.01-0.03|^\circ\text{C}$.

From the analysis of the depth error (Fig. 11), an average temperature uncertainty $|\delta T| \sim 0.03-0.05^\circ\text{C}$ below 200 m depth has been deduced, but the existence of a sometime strong disagreement in the upper region is confirmed. If the results of the calibration are combined with the other uncertainties reviewed in this paper, the expected range is $|\delta T_{\text{tot}}| \sim 0.05-0.10^\circ\text{C}$, in good agreement with in situ measurements based on CTD and MedArgo profiles (Poulain, private communication, 2005).

The temperature uncertainty within the profile for Sippican T4/T6 and DB probes deduced from this test can be summarized as follows:

- $|\delta T| \leq 0.10^\circ\text{C}$ from the surface down to the thermocline, if it exists;
- $|\delta T| \leq 0.50^\circ\text{C}$ where the thermocline starts (if any), and proportional to its strength (with possible spikes up to 3.0°C , but over a layer of a few metres);
- $|\delta T| \leq 0.07^\circ\text{C}$ below the base of the thermocline ($|\delta T| \leq 0.14^\circ\text{C}$ in regions where identified thermal structures occur).

5 Concluding remarks

In this paper, contemporaneous and co-located CTD and XBT temperature profiles from the Western Mediterranean Sea are compared in order to evaluate the performances of T4 and DB probes manufactured by Sippican.

As a preliminary step, the concept of acquisition time is introduced to analyze time ordered temperature values (depth ordered in previous standard analyses). The extended data acquisition for XBT probes, which has been the standard procedure within MFS-TEP and ADRICOSM since 2003, is presented and the reliability of the extended profiles has been verified. Acquisition time values increased by about 20% without significant variation of the quality of recorded temperatures have been successfully measured for several types of probes. In addition, DB and T7 probes have also been dropped from ships moving faster than nominal maximum speed, and with good quality of recorded values throughout the whole profile.

The evaluation of the influence of the initial probe mass on the acquisition time has been impossible, due to the variability of the weight of each probe component and of the linear density of the copper wire, which could produce differences up to 35 m in wire length (or more than 5 s in acquisition time).

The twin drops from different height during the same CTD cast have given uncertain indications about the influence of the launching height on the motion in the near surface layer. It is hard to separate the contribution due to the height of launching position from the one due to weight and probe-to-probe variability, each probe having a random and unpredictable behaviour.

The calibration of the XBT probes and the data acquisition system at NURC Laboratories strengthens confidence in XBT measurements: the range of the obtained differences is $0.04-0.08^\circ\text{C}$, and the probe-to-probe variability is $0.01-0.03^\circ\text{C}$. All the calibrated probes measure temperatures higher than the real values and the results show slightly greater differences with smaller variability than in earlier calibrations done at NURC.

A significant part of the problems occurring in the near surface layer has been explained in terms of the response time of the acquisition system, i.e. the time needed to measure temperature values within the standard probe accuracy.

The thermal structures in the upper region are better reproduced by computing an empirical value of the response time (0.3 s), and eliminating the first three recorded values. This means that the fourth value in the original acquisition sequence has been considered the first one, and the remaining part of the profile has been shifted up by 2 m. This empirical solution seems to be successfully extendable to all XBT types.

It has been verified that the fall rate equation with IGOSS coefficients (Table 2) describes the motion of the analysed XBT probes in a reasonable way, but a non-negligible difference, depending on the XBT type, frequently occurs. The discrepancy in depth is more evident for T4 probes. Therefore, new fall rate coefficients have been computed in a new way, because of difficulties in applying the method proposed by Hanawa et al. (1994, 1995) due to the high homogeneity in Mediterranean seawater. T4 profiles show a better agreement with CTD profiles only if the A coefficient is significantly reduced: thermal structures occur at a depth smaller than the values obtained by using the previous procedures and IGOSS fall rate coefficients (differences up to 20 m). On the contrary, DB probes present smaller discrepancy in the depth of thermal structures and the maximum values differ by no more than few metres.

The calculated B coefficients are within the range of variability allowed by the IGOSS Report for each specific type. The influence of the B coefficient should be more evident in the final part of the extended acquisition, due to motion for a time longer than usual when the probes are lighter, but available results show that no significant differences in the XBT motion appear below the nominal terminal depth. Recorded temperatures are reliable down to about 550 m depth for T4 and about 920 m depth for DB probes.

New fall rate coefficients have been calculated for XBT profiles dropped in the Western Mediterranean Sea, and their use is suggested for probes of the same type dropped in the same or in neighbouring areas, having similar temperature and salinity values. Any extension to probes dropped in the Eastern Mediterranean Sea would be rash without *in situ* specific comparisons, because of different water mass characteristics of the Levantine basin. Therefore, a XBT-CTD comparison in these areas is needed to complete the screening of the Mediterranean Sea.

The analysis of the temperature difference profiles for T4 and DB probes has shown a residual component, whose value below 100 m depth can be reproduced well by a linear function of the depth. The constant term, which should be related to the intrinsic properties of the probe and data acquisition system, agrees substantially with those cited in the literature, and with the values from the calibration. The temperature coefficient (Table 5) seems to allow the description of most of the residual temperature error and other unknown and probe-specific unpredictable effects. In such a way, the mean temperature difference between XBT and CTD measurements becomes symmetric and decreases.

Acknowledgements. The authors acknowledge M. Astraldi (CNR-ISMAR, Sez. Oceanografia Fisica, Lerici, Italia) for the extensive use of CTD profiles, S. Kizu (Dept. of Geophysics, Graduate School of Science, Tohoku University, Sendai, Japan) for many suggestions, P. Zanasca (NURC, La Spezia, Italia) for discussions and the use of his own results, and the referees and the editor for their thoughtful comments for improving the manuscript. This work has been funded by Italian Ministries of Environment and of Foreign Affairs, and UNESCO-IOC (ADRICOSM projects), and by European Commission – DG Research under contract EVK3-CT-20-00075 (MFS-TEP project).

Edited by: J. A. Johnson

References

- AODC: Guide to MK12 – XBT System (Including Launching, returns and faults), Australian Oceanographic Data Centre (AODC), METOC Services, 1–63, 1999.
- AODC: Expendable Bathythermographs (XBT) delayed mode, Quality control manual, Australian Oceanographic Data Centre (AODC), Data Management Group, Technical Manual 1/2001, 1–24, 2001.
- AODC: Marine QC. Australian Oceanographic Data Centre (AODC), Data Management Group, Technical Manual 1/2002, 1–61, 2002.
- Budéus, G. and Krause, G.: On cruise calibration of XBT probes, *Deep-Sea Res.*, 40, 1359–1363, 1993.
- Cook, S. and Sy, A.: Best guide and principles manual for the Ships Of Opportunity Program (SOOP) and EXpendable Bathythermograph (XBT) operations, Prepared for the IOC-WMO-3rd Session of the JCOMM Ship of Opportunity Implementation Panel (SOOPIP-III), March 28–31, 2000, La Jolla, California, USA, 1–26, 2001.
- Fedorov, K. N., Ginzburg, A. I., and Zatsepen, A. G.: Systematic differences in isotherm depths derived from XBT and CTD data, *POLYMODE News*, 50(1), 6–7, 1978.
- Flierl, G. and Robinson, A. R.: XBT measurements of the thermal gradient in the MODE eddy, *J. Phys. Oceanogr.*, 7, 300–302, 1977.
- Georgi, D., Dean, J., and Chase, J.: XBT probe-to-probe thermistor temperature variability, *POLYMODE News*, 71(1), 5–9, 1979.
- Georgi, D., Dean, J., and Chase, J.: Temperature calibration of expendable bathythermographs, *Ocean Engineering*, 7, 491–499, 1980.
- Green, A. W.: Bulk dynamics of the Expendable Bathythermograph (XBT), *Deep-Sea Res.*, 31, 415–426, 1984.
- Hallock, Z. R. and Teague, W. J.: The fall rate of the T7 XBT, *J. Atmos. Oceanic Technol.*, 9, 470–483, 1992.
- Hanawa, K., Rual, P., Bailey, R., Sy, A., and Szabados, M.: Calculation of new depth equations for Expendable Bathythermographs using a temperature-error-free method (Application to Sippican/TSK T7, T6 and T4 XBTs), Intergovernmental Oceanographic Commission (IOC) Technical Series 42, 1–46, 1994.
- Hanawa, K., Rual, P., Bailey, R., Sy, A., and Szabados, M.: A new depth-time equation for Sippican or TSK T7, T6 and T4 expendable bathythermographs (XBT), *Deep-Sea Res. Part I*, 42(8), 1423–1451, 1995.

- Hanawa, K. and Yoshikawa, Y.: Re-examination of the depth error in XBT data, *J. Atmos. Oceanic Technol.*, 8, 422–429, 1991.
- Hanawa, K. and Yasuda, T.: New detection method for XBT depth error and relationship between the depth error and coefficients in the depth-time equation, *J. Oceanogr.*, 48, 221–230, 1992.
- Heinmiller, R. H., Ebbesmeyer, C. C., Taft, B. A., Olson, D. B., and Nikitin, O. P.: Systematic Errors in Expendable Bathythermograph (XBT) Profiles, *Deep-Sea Res.*, 30(11A), 1185–1197, 1983.
- Kizu, S. and Hanawa, K.: Start-up transient of XBT measurement, *Deep-Sea Res. Part I*, 49, 935–940, 2002a.
- Kizu, S. and Hanawa, K.: Recorder-Dependent Temperature error of Expendable Bathythermograph, *J. Oceanogr.*, 58(3), 469–476, 2002b.
- Maillard, C. and Fichaut M.: MEDAR-MEDATLAS Protocol. Part I. Exchange format and quality checks for observed profiles, *Rap. Int. TMSI/IDM/SISMER/SIS00-084*, 1–49, 2001.
- Manzella, G. M. R., Scoccimarro, E., Pinardi, N., and Tonani, M.: Improved near real time data management procedures for the Mediterranean ocean Forecasting System – Voluntary Observing Ship Program, *Ann. Geophys.*, 21, 49–62, 2003, <http://www.ann-geophys.net/21/49/2003/>.
- McDowell, S.: A note on XBT accuracy, *POLYMODE News*, 29(1), 4–8, 1977.
- Roemmich, D. and Cornuelle, B.: Digitization and calibration of the expendable bathythermograph, *Deep-Sea Res.*, 34, 299–307, 1987.
- Seaver, G. A. and Kuleshov, S.: Experimental and analytical error of Expendable bathythermograph, *J. Phys. Oceanogr.*, 12, 592–600, 1982.
- Singer, J.: On the error observed in electronically digitised T7 XBT data, *J. Atmos. Oceanic Technol.*, 7, 603–611, 1990.
- Stegen, G. R., Delisi, D. P., and Van Colln, R. C.: A portable, digital recording, expendable bathythermograph (XBT) system, *Deep-Sea Res.*, 22, 447–453, 1975.
- Sy, A.: XBT measurements, in: WOCE Operations Manual, WHP Operation and Methods, WHPO 91-1, WOCE Report 68/91, 1–19, 1991.
- Thadathil, P., Ghosh, A. K., and Muraleedharan, P. M.: An evaluation of XBT depth equations for the Indian Ocean, *Deep-Sea Res. Part I*, 45, 819–827, 1998.
- Thadathil, P., Saran, A. K., Gopalakrishna, V. V., Vethamony, P., Araligidat, N., and Bailey, R.: XBT fall rate in waters of extreme temperature: a case study in the Antarctic Ocean, *J. Atmos. Oceanic Technol.*, 19, 391–396, 2002.